Cerebrovascular reactivity in retinal vasculopathy with cerebral leukoencephalopathy and systemic manifestations

Hoogeveen, E.S.; Pelzer, N.; Ghariq, E.; Osch, M.J.P. van; Dahan, A.; Terwindt, G.M.; Kruit, M.C.

Original Article

JCBFM

Journal of Cerebral Blood Flow & Metabolism
2021, Vol. 41(4) 831–840

DOI: 10.1177/0271678X20929430
journals.sagepub.com/home/jcbfm


Cerebrovascular reactivity in retinal vasculopathy with cerebral leukoencephalopathy and systemic manifestations

Evelien S Hoogeveen[1], Nadine Pelzer[2], Eidrees Ghariq[1,3], Matthias JP van Osch[1,3], Albert Dahan[4], Gisela M Terwindt[2,*] and Mark C Kruit[1,*]

Abstract

Retinal Vasculopathy with Cerebral Leukoencephalopathy and Systemic manifestations (RVCL-S) is a small vessel disease caused by *TREX1* mutations. RVCL-S is characterized by retinal vasculopathy and brain white matter lesions with and without contrast enhancement. We aimed to investigate cerebrovascular reactivity (CVR) in RVCL-S. In this cross-sectional observational study, 21 RVCL-S patients, 23 mutation-negative family members, and 31 healthy unrelated controls were included. CVR to a hypercapnic challenge was measured using dual-echo arterial spin labeling magnetic resonance imaging. Stratified analyses based on age were performed. We found that CVR was decreased in gray and white matter of RVCL-S patients compared with family members and healthy controls (ANCOVA; $P < 0.05$ for all comparisons). This was most noticeable in RVCL-S patients aged $\geq$40 years (ANCOVA, $P < 0.05$ for all comparisons). In RVCL-S patients aged $<$ 40 years, only CVR in white matter was lower when compared to healthy controls ($P < 0.05$). Gray matter CVR was associated with white matter lesion volume in RVCL-S patients ($r = -0.527$, $P = 0.01$). In conclusion, impaired cerebrovascular reactivity may play an important role in the pathophysiology of RVCL-S and may be an useful early biomarker of cerebrovascular disease severity.

Keywords

Cerebrovascular circulation, cerebrovascular disorders, leukoencephalopathies, magnetic resonance imaging, mutation

Received 1 November 2019; Revised 5 April 2020; Accepted 20 April 2020

Introduction

Retinal Vasculopathy with Cerebral Leukoencephalopathy and Systemic manifestations (RVCL-S) is an autosomal dominantly inherited small vessel disease caused by heterozygous C-terminal frameshift mutations in the *TREX1* gene.[1,2] How exactly *TREX1* mutations lead to disease is still unresolved, but vasculopathic changes seem the cornerstone behind most features. These features include almost always vascular retinopathy and multifocal brain white matter lesions (WMLs). Brain WMLs may show contrast enhancement, implicating disruption of the blood–brain barrier of the local vasculature. Brain WMLs may have associated vasogenic and/or cytotoxic edema and may change in size, incidentally leading to

[1]Department of Radiology, Leiden University Medical Center, Leiden, The Netherlands
[2]Department of Neurology, Leiden University Medical Center, Leiden, The Netherlands
[3]C.J. Gorter Center for High Field MRI, Leiden University Medical Center, Leiden, The Netherlands
[4]Department of Anesthesiology, Leiden University Medical Center, Leiden, The Netherlands

*These authors contributed equally to this work.

Corresponding author:
Mark C Kruit, Department of Radiology, Leiden University Medical Center, Albinusdreef 2, Postbus 9600, 2300 RC Leiden, The Netherlands.
Email: m.c.kruit@lumc.nl

the formation of a "pseudotumor". Other RVCL-S features include migraine, kidney and liver disease, anemia, hypertension, subclinical hypothyroidism, and Raynaud's phenomenon.[1–6]

The underlying systemic vasculopathy of medium and small caliber arteries in RVCL-S is pathologically characterized by irregular thickening and splitting of basement membranes, smooth muscle cell and pericyte degeneration, fibrinoid necrosis, adventitial fibrosis, and mural hyalinization with collagenous material.[2] These changes lead to vessel wall thickening, luminal narrowing, and vessel obliteration. Brain WMLs around such blood vessels are characterized by areas of ischemic necrosis, reactive chronic inflammatory cell infiltrates, reactive astrocytosis, and myelin and axonal loss.[2]

A previous study showed reduced vascular reactivity and increased vascular stiffness in the brachial arteries of RVCL-S patients.[7] But up until now, no study has evaluated cerebrovascular reactivity (CVR) in RVCL-S. We hypothesized that *TREX1*-related vasculopathy gradually leads to global reduced CVR. CVR is known as the cerebrovascular reserve capacity and is a marker for cerebrovascular health. It can be measured as change in cerebral blood flow (CBF) to a hypercapnic stimulus.[8,9] While blood oxygenation level dependent (BOLD) magnetic resonance imaging (MRI) has been the most commonly used readout marker, it is not a direct measure of CBF. Arterial spin labeling (ASL) MRI directly measures CBF but a drawback is that it suffers from a low signal-to-noise ratio. ASL-MRI with a dual-echo readout module provides simultaneous acquisition of ASL and BOLD images.

To test the hypothesis of reduced CVR in RVCL-S patients, we assessed global and regional CVR to hypercapnia using ASL and BOLD MRI in RVCL-S patients with a proven *TREX1* mutation and compared results to *TREX1* mutation-negative family members and healthy unrelated controls.

Materials and methods

Participants

We included 47 family members from three Dutch RVCL-S families. *TREX1* mutation status was determined in all individuals: 23 subjects had a mutation in the *TREX1* gene and 24 did not. The genetic status of individuals was not disclosed to participants, unless clinically requested by a clinical geneticist or neurologist. Family members who proved not to have a *TREX1* mutation served as a control group. Thirty-two healthy volunteers were included as an additional control group to exclude that other genetic variants than the mutations in the *TREX1* gene might influence results for the family members without a *TREX1* mutation. Exclusion criteria were age younger than 18 years, severe asthma and chronic obstructive pulmonary disease, and any contraindication to MRI. Additional exclusion criteria for healthy controls were (i) primary headache syndrome, (ii) history of transient ischemic attack or ischemic or hemorrhagic brain infarct, (iii) presence of multiple sclerosis, (neuro-)systemic lupus erythematosus, brain tumor, vascular malformation, or vasculitis, (iv) presence of hypertension, (v) presence of diabetes mellitus, (vi) history of severe carotid artery stenosis, (vii) kidney or liver disease, (viii) Raynaud's syndrome, and (ix) presence of malignancy. All participants were asked not to eat or drink (except for water) at least four hours prior to the measurements and to refrain from smoking at least two hours before measurements. All participants were scanned between 17:00 and 21:00 h. The medical ethics committee of the Leiden University Medical Center approved the study, and all participants gave written, informed consent. Study was performed according to guidelines of the Declaration of Helsinki.

MRI data acquisition

All imaging procedures were performed on a 3.0 T clinical MRI system (Philips, Best, The Netherlands). A dynamic dual-echo pseudo continuous ASL scan was employed to monitor the response to the CO_2 challenge with the following scan parameters: TR = 4100 ms, TE1/TE2 = 13/35 ms, label duration/post-label delay = 1650/1525 ms, multi-slice single shot EPI with background suppression (inversion pulses at 1680 and 2760 ms), 15 slices, voxel-size = 3 × 3 × 7 mm, 75 pairs of label and control images, ascending slice acquisition-order. The labeling plane was placed perpendicular to the internal carotid arteries and the vertebral arteries. We further acquired a dual-echo M0 scan (TR = 2000 ms, TE1/TE2 = 13/35 ms, resolution of 80 × 80, flip angle 90°, voxel-size 3 × 3 mm, 15 slices of 7 mm), a $T1_{blood}$ scan (TR = 150 ms, TE = 11 ms, resolution 240 × 240, flip angle 95°, voxel-size 1 × 1 mm, 1 slice of 2 mm),[10] and a 3D T1-weighted anatomical scan (TR = 9.8 ms, TE = 4.6 ms, flip angle 8°, voxel-size 1.15 × 1.15 mm, 130 slices of 1.2 mm).

CBF was calculated using the following equation[11]

$$\mathrm{CBF} = \frac{6000 \cdot \lambda \cdot \Delta\mathrm{ASL} \cdot e^{\left(\frac{\mathrm{PLD}}{\mathrm{T1blood}}\right)}}{2 \cdot a \cdot \mathrm{T1blood} \cdot \mathrm{M0} \cdot \left(1 - e^{\left(-\frac{\tau}{\mathrm{T1blood}}\right)}\right)}$$

where partition coefficient $\lambda = 0.9$; post-label delay (PLD) = 1.525 s (for the first acquired slice; the PLD was adjusted for subsequent slices according to the inter-slice interval) and $\tau = 1.65$ s. ΔASL is the

difference in signal intensity of the control image minus label image. M_0 is the longitudinal magnetization of arterial blood and was obtained by the M0 scan. To correct for potential differences in hematocrit, the T1 relaxation time of blood was obtained from the $T1_{blood}$ scan.[10]

CO_2 reactivity experiment

During the MRI session, subjects wore a close-fitting gas mask over the mouth and nose with a constant gas delivery at 50 L/min. Gas composition was monitored using an O_2 and CO_2 analyzer (Datex Capnomac Ultima^{TM}). The paradigm of this 10-min CO_2 reactivity experiment consisted of three alternating blocks of normocapnia (21% O_2, 79% N_2) with two blocks of hypercapnia (21% O_2, 74% N_2, 5% CO_2). Values for end-tidal partial pressure of CO_2 ($PetCO_2$) were extracted from respiratory data. Blood pressure and heart-rate were measured during 0, 3, 5, 7, and 9 min. Before MRI measurements started, a test run of the CO_2 experiment was completed outside the MRI room.

Post-processing of imaging data

For the measurement of WMLs, tools of the FSL software package (Functional MRI of the Brain (FMRIB) Software Library v5, www.fmrib.ox.ac.uk/fsl) were used.[12] T1-weighted and Fluid Attenuated Inversion Recovery (FLAIR) images were brain extracted using the brain extraction tool and co-registered using FMRIB's linear image registration tool to the MNI standard space (MNI152, Montreal Neurological Institute). WMLs in a conservative MNI white matter mask were automatically identified using a threshold of three standard deviations above the mean FLAIR signal intensity.

An in-house MATLAB (MathWorks, Natick, MA, USA) script was used to separate the acquired dual-echo pseudo continuous ASL data into distinct ASL and BOLD files. Motion correction was performed using the software Statistical Parametric Mapping (v12, http://www.fil.ion.ucl.ac.uk/spm). Further preprocessing of 3D T1-weighted, ASL and BOLD images was performed using FSL.[12] First, images were brain-extracted using the brain extraction tool. CBF was based on the sinc-subtracted first echo images, while BOLD was based on the surround averaged second echo images, i.e. for every image (control or label), a weighted average of the image and its two neighboring images was taken. The BOLD images were high-pass filtered (240 s) and ASL and BOLD images were spatially smoothed using a Gaussian kernel (full-width half-maximum = 5 mm). The ASL and BOLD were registered to the 3D T1-weighted images using the linear registration tool. The 3D T1-weighted image was then transformed using FMRIB's nonlinear image registration tool into the MNI152 space. ASL and BOLD images were nonlinearly registered to the MNI152 template by applying the transformation parameters of the normalized 3D T1-weighted images. These transformations were concatenated and then inverted to enable the conversion of gray and white matter masks obtained from tissue segmentation of the T1-weighted images using FMRIB's automated segmentation tool, and the WML mask into the functional space of every subject. The WML mask was used to mask the gray and white matter segmentations to avoid inclusion of WML.

CO_2 CVR calculation

CBF and BOLD time-courses were extracted from the gray matter and the normal appearing white matter using the gray and white matter segmentation images (without WMLs). Because of the low signal-to-noise ratio of ASL in white matter, white matter CVR was not evaluated for CBF. The corresponding sampled $PetCO_2$ waveform was temporally aligned to the gray matter BOLD time-course by computing the delay between the $PetCO_2$ measures and changes in BOLD signal. CVR was calculated performing a least-squares fit of the CBF or BOLD signals and the $PetCO_2$ time-course to a linear model. The computed slope was normalized to the baseline CBF or BOLD signal to express CVR in units of %ΔCBF/mmHg CO_2 or %ΔBOLD/mmHg CO_2. Baseline CBF was defined as the mean CBF during the three normocapnic blocks, while excluding the first 16 s from every block. Likewise, normocapnic and hypercapnic $PetCO_2$ values were defined from the normocapnic or hypercapnic blocks respectively, while excluding the first 16 s of every block.

Voxel-wise maps of CVR were acquired by performing a least-squares fit of the CBF and BOLD maps to the shifted $PetCO_2$ time-course.

Statistical analysis

Data are presented as mean ± SD or as number (percentage). For the demographic and clinical continuous variables, differences between groups were assessed by one-way analysis of variance; categorical variables were compared by the Kruskal–Wallis test. CVR data were compared between RVCL-S patients, mutation-negative family members, and healthy controls using analyses of covariance controlling for age and sex. To determine whether CVR is altered before development of characteristic RVCL-S features, analyses were repeated after stratification by age, i.e. splitting the subjects into a group aged < 40 years (generally without

or with only few clinical RVCL-S features) and aged ≥40 years (usually with characteristic clinical RVCL-S features).[2,6]

WML volumes were skewed and therefore logarithmically transformed. Correlation analyses were used to assess the association between CVR and WML volumes in the RVCL-S patients. Two-tailed P-values < 0.05 were considered significant.

For voxel-wise statistics, the FSL randomize tool with threshold-free cluster enhancement was used to perform permutation-based nonparametric testing ($n = 5000$ permutations). Voxel-wise analyses of CVR were performed using a whole brain (gray and white matter) approach on the BOLD data. Voxel-wise analyses of CVR_{CBF} were restricted to gray matter because of the low signal-to-noise ratio of ASL in white matter. In order to exclude RVCL-S lesions from the analyses, the lesion masking tool was applied using the individual WML masks. Significance was set at a family wise error corrected $P < 0.05$.

Results

Of 47 RVCL-S family members, 23 subjects had a *TREX1* mutation. Two RVCL-S mutation carriers, one mutation-negative family member, and one healthy control were excluded from analyses because of coincidental (RVCL-S unrelated) findings on MRI or incomplete measurements. Thus, 21 RVCL-S patients, 23 mutation-negative family members, and 31 healthy controls were included for analyses. Baseline characteristics were compared (Table 1) and showed that hypertension was different between the groups ($P = 0.002$; Table 1), mainly due to fact that hypertension was an exclusion criterion for healthy controls and hypertension is a feature of RVCL-S. Age, sex, BMI, and WMLs were similar between the groups.

RVCL-S patients had on an average a higher mean normocapnic CBF and higher systolic and diastolic blood pressure during normocapnia and hypercapnia compared to their mutation-negative family members and healthy controls (Table 2). $PetCO_2$ values were comparable between the groups. CVR in gray matter as measured with both CBF (CVR_{CBF}) and BOLD (CVR_{BOLD}) were different between the three groups after controlling for age and sex (respectively $F(2, 70) = 3.54$, $P = 0.03$; $F(2, 70) = 6.66$, $P = 0.002$; Table 3). Post-hoc tests revealed that RVCL-S patients had lower gray matter CVR_{CBF} and CVR_{BOLD} compared to both their mutation-negative family members and to healthy controls. CVR_{BOLD} in the normal appearing white matter was also different between the groups ($F(2, 70) = 10.33$, $P < 0.001$); this was lower in RVCL-S patients compared to their mutation-negative family members and compared to healthy controls (Table 3).

In the RVCL-S patients aged ≥40 years, gray matter CVR_{CBF} and CVR_{BOLD} (respectively $F(2, 44) = 4.31$, $P = 0.02$; $F(2, 44) = 6.30$, $P = 0.004$) were lower compared to both mutation-negative family members and healthy controls in the same age group (Table 3). Similarly, white matter CVR_{BOLD} ($F(2, 44) = 8.50$, $P = 0.001$) was lower in the RVCL-S patients aged ≥40 years compared to both mutation-negative family members and healthy controls. In the younger age group of RVCL-S patients (< 40 years), only white matter CVR_{BOLD} ($F(2, 21) = 7.50$, $P = 0.003$) was lower compared to healthy controls but not when compared to mutation-negative family members. Gray matter CVR_{CBF} ($F(2, 21) = 0.50$, $P = 0.6$) and CVR_{BOLD} $F(2, 21) = 1.92$, $P = 0.2$) were not different between the younger groups.

The relation of CVR with age in the different groups is illustrated in Figure 1. Gray matter CVR_{CBF} was significantly associated with age in RVCL-S patients ($r = -0.688$, $P = 0.001$), but not in mutation-negative family members ($r = 0.085$, $P = 0.7$) or healthy controls ($r = -0.247$, $P = 0.2$). Gray matter CVR_{BOLD} was significantly associated with age in RVCL-S patients ($r = -0.434$, $P = 0.049$) and healthy controls ($r = -0.473$, $P = 0.007$) but not in mutation-negative family

Table 1. Baseline characteristics of study participants ($n = 75$).

	RVCL-S ($n = 21$)	Family members ($n = 23$)	Healthy controls ($n = 31$)	*P*-value
Age (y)	44.5 ± 15	43.4 ± 12	45.4 ± 14	NS
Female, *n*(%)	11 (52)	11 (52)	18 (58)	NS
Body mass index (kg/m^2)	23.7 ± 3	25.9 ± 4	23.8 ± 3	NS
Hypertension, *n*(%)	8 (43)	6 (22)	0	0.002
WMLs (mL), median (range)	0.4 (0–26.8)	0.4 (0.1–2.5)	0.8 (0–7.2)	NS[a]

Note: Data represent mean ± SD unless specified otherwise.
WMLs: white matter lesions; RVCL-S: Retinal Vasculopathy with Cerebral Leukoencephalopathy and Systemic manifestations.
[a]Kruskal–Wallis test.

Table 2. Blood pressure, $PetCO_2$, and CBF values at normocapnia and hypercapnia in RVCL-S patients, mutation-negative family members, and healthy controls.

	RVCL-S ($n=21$)	Family members ($n=23$)	Healthy controls ($n=31$)	*P*-value
Systolic BP, normocapnia (mmHg)	132.6 ± 19	125.6 ± 14[a]	125.0 ± 13[a]	0.02
Diastolic BP, normocapnia, (mmHg)	76.0 ± 11	77.4 ± 8	73.2 ± 7	0.05
Systolic BP, hypercapnia (mmHg)	135.9 ± 24	128.7 ± 15	128.0 ± 14[a]	0.03
Diastolic BP, hypercapnia (mmHg)	80.1 ± 12	81.8 ± 9	76.5 ± 8[a]	0.03
$PetCO_2$, normocapnia (mmHg)	37.6 ± 3	38.3 ± 4	38.5 ± 3	0.33
$PetCO_2$, hypercapnia (mmHg)	46.8 ± 3	47.5 ± 3	48.2 ± 2	0.07
Δ $PetCO_2$ (mmHg)	9.2 ± 1	9.2 ± 1	9.7 ± 1	0.35
CBF, normocapnia (mL/100 g/min)	55.3 ± 8	49.3 ± 8[a]	46.3 ± 6[b]	<0.001

BP: blood pressure; $PetCO_2$: partial pressure of end tidal CO_2; CBF: cerebral blood flow; RVCL-S: Retinal Vasculopathy with Cerebral Leukoencephalopathy and Systemic manifestations.
Note: *P*-values are calculated using ANCOVA corrected for age and sex.
[a]$P < 0.05$ compared to RVCL-S patients.
[b]$P < 0.001$ compared to RVCL-S patients.

Table 3. Cerebrovascular reactivity in RVCL-S patients, mutation-negative family members, and healthy controls.

	RVCL-S	Family member	Healthy control	*P*-value
All, *n*	21	23	31	
Gray matter				
CVR_{CBF}	2.9 ± 1.0	3.6 ± 1.2[a]	3.4 ± 1.0[a]	**0.03**
CVR_{BOLD}	0.16 ± 0.05	0.19 ± 0.04[a]	0.18±0.04[a]	**0.002**
White matter				
CVR_{BOLD}	0.06 ± 0.02	0.08 ± 0.02[b]	0.08 ± 0.02[b]	**<0.001**
< 40 years, *n*	10	6	10	
Gray matter				
CVR_{CBF}	3.6 ± 1.0	3.7 ± 0.4	3.8 ± 1.3	0.6
CVR_{BOLD}	0.18 ± 0.04	0.20 ± 0.05	0.22 ± 0.05	0.2
White matter				
CVR_{BOLD}	0.07 ± 0.01	0.07 ± 0.02	0.09 ± 0.02[a]	**0.003**
≥ 40 years, *n*	11	17	21	
Gray matter				
CVR_{CBF}	2.3 ± 0.8	3.6 ± 1.4[a]	3.2 ± 0.9[a]	**0.02**
CVR_{BOLD}	0.13±0.05	0.19±0.03[a]	0.16 ± 0.03[a]	**0.004**
White matter				
CVR_{BOLD}	0.05 ± 0.03	0.08 ± 0.02[b]	0.08 ± 0.02[a]	**0.001**

RVCL-S: Retinal Vasculopathy with Cerebral Leukoencephalopathy and Systemic manifestations; CVR: cerebrovascular reactivity; CBF: cerebral blood flow; BOLD: blood oxygenation level dependent.
Notes: Data represent mean ± SD. *P*-values are calculated using ANCOVA corrected for age and sex.
[a]$P < 0.05$ compared to RVCL-S patients.
[b]$P < 0.001$ compared to RVCL-S patients.

members ($r=-0.254$, $P=0.2$). White matter CVR_{BOLD} was not associated with age in RVCL-S patients ($r=-0.275$, $P=0.2$), mutation-negative family members ($r=0.286$, $P=0.2$), or healthy controls ($r=-0.293$, $P=0.1$). An outlier was found in the mutation-negative family member group for gray matter CVR_{CBF} and white matter CVR_{BOLD}. Exclusion of this outlier changed the direction of the association between CVR_{CBF} and age in mutation-negative family members ($r=-0.260$, $P=0.2$), but otherwise did not influence the results (data not shown).

We assessed the association between WML volume and CVR within the RVCL-S group. The association between WML volume and gray matter CVR_{BOLD} was

significant ($r = -0.527$, $P = 0.01$) and there was a trend for gray matter CVR_{CBF} ($r = -0.408$; $P = 0.07$). The association between WML volume and white matter CVR_{CBF} did not reach statistical significance ($r = -0.317$, $P = 0.2$) (Figure 2).

After exclusion of WMLs, voxel-wise analyses showed a significant reduction in CVR in multiple normal appearing brain areas, most notably in the frontal and parietal white matter, the thalamus and midbrain, and frontal, insular and precuneal cortical areas of RVCL-S patients compared to both mutation-negative family members and healthy controls (Figure 3). In gray matter, there is considerable overlap in the voxel-wise CVR_{CBF} and CVR_{BOLD} statistical maps. However some regional differences can be appreciated. CVR_{BOLD} findings are more explicit in the frontal regions, while CVR_{CBF} changes are more present in the occipital regions (Figure 3).

Discussion

The results of the present study indicate that RVCL-S patients are associated with impaired CVR compared with their mutation-negative family members and healthy controls. This was most notable in RVCL-S patients aged $\geq$40 years, when clinical symptoms usually manifest.[2,6] However, also RVCL-S patients < 40 years showed reduced white matter CVR compared with healthy controls. Gray matter CVR was inversely associated with WML volume in RVCL-S patients. Collectively, our findings support the notion that RVCL-S *TREX1* mutations are associated with altered CVR which in turn may promote development of WMLs in RVCL-S.

CVR defines the ability to change CBF in response to vasodilatory stimuli. Increased arterial CO_2 levels lead to vascular relaxation and hence vasodilatation.[13,14] A previous study showed that CO_2 CVR can be considered a surrogate marker of cerebrovascular endothelial function.[15] Thus, our findings of reduced CO_2 CVR suggests endothelial involvement in RVCL-S patients. Our data add to previous studies in RVCL-S families where RVCL-S patients exhibited a decreased extra-cranial flow-mediated dilation corresponding with impaired peripheral endothelial function[7] and had elevated levels of circulating endothelial markers,[16] thereby suggesting an important role of the endothelium in the pathophysiology of RVCL-S. The current findings indicate a similar behavior of the extra- and intracranial vasculature in RVCL-S.

Although characteristic enhancing RVCL-S WMLs are mostly seen after the age of 40 years, small focal WMLs are also observed at an age when age-related WMLs are infrequent.[2] We hypothesize that impaired white matter CVR leads to development of WMLs by poorer responses when metabolic needs require a higher blood supply. Impaired CVR may reflect the *TREX1*-associated vessel wall changes characterized by multi-laminated capillary basement membranes and luminal narrowing.[2,3] These vessel wall changes may also lead to development of WMLs by injury of the surrounding brain tissue by toxic agents which pass a locally impaired blood–brain barrier.

Gray matter CVR was only impaired in RVCL-S patients $\geq$40 years, but not in the younger group. Neuropathology findings in RVCL-S show vasculopathic changes notably in medium and small caliber arteries and veins in the white matter with typical sparing of cortical gray matter vessels.[5] Based on our findings, the cortical gray matter vessels are probably affected in later disease stages of RVCL-S. We also know from literature that other RVCL-S features such as chronic hypertension and anemia may contribute to decreased gray matter CVR.[17,18] The increased mean baseline CBF in the RVCL-S group might also be explained by anemia or increased blood pressure.[18,19] Since hypertension and anemia are features of RVCL-S, we could not correct for this in our analyses nor can we exclude that this may be (one of the) causes of the decreased CVR.

Although only gray matter CVR_{BOLD} was correlated with WML volume, a trend was observed in gray matter CVR_{CBF} (Figure 2). Moreover, using additional voxel-wise analyses, we showed that CVR is mainly reduced in the (normal appearing) white matter of the frontoparietal regions (Figure 3), where RVCL-S lesions predominantly develop.[2,20]

In the past, BOLD has been the most commonly used readout marker for assessing CVR. However, a well-known concern is that the BOLD signal is not a direct measure of CBF but is sensitive to the combined effect of CBF, cerebral blood volume, and cerebral metabolic rate of oxygen. In patients with known small vessel pathology, this might limit our ability to interpret the results. ASL-MRI directly measures CBF but a drawback is that it suffers from a lower signal-to-noise ratio. Therefore, ASL and BOLD are complementary to each other, which was why in our study, a dual echo ASL sequence was employed. In Table 3, both gray matter CVR_{CBF} and CVR_{BOLD} were impaired in RVCL-S patients. This suggests that CVR_{BOLD} with a hypercapnic stimulus is largely related to changes in CBF and that both measures can be used interchangeably in RVCL-S.

The voxel-wise analyses in Figure 3 show some regional differences between the statistical maps of CVR_{CBF} and CVR_{BOLD}. This can be partly explained by the fact that for the voxel-wise CVR_{BOLD} analyses, both gray and white matter were included, whereas the white matter was masked out for the CVR_{CBF} analyses. In gray matter, there is considerable overlap in the

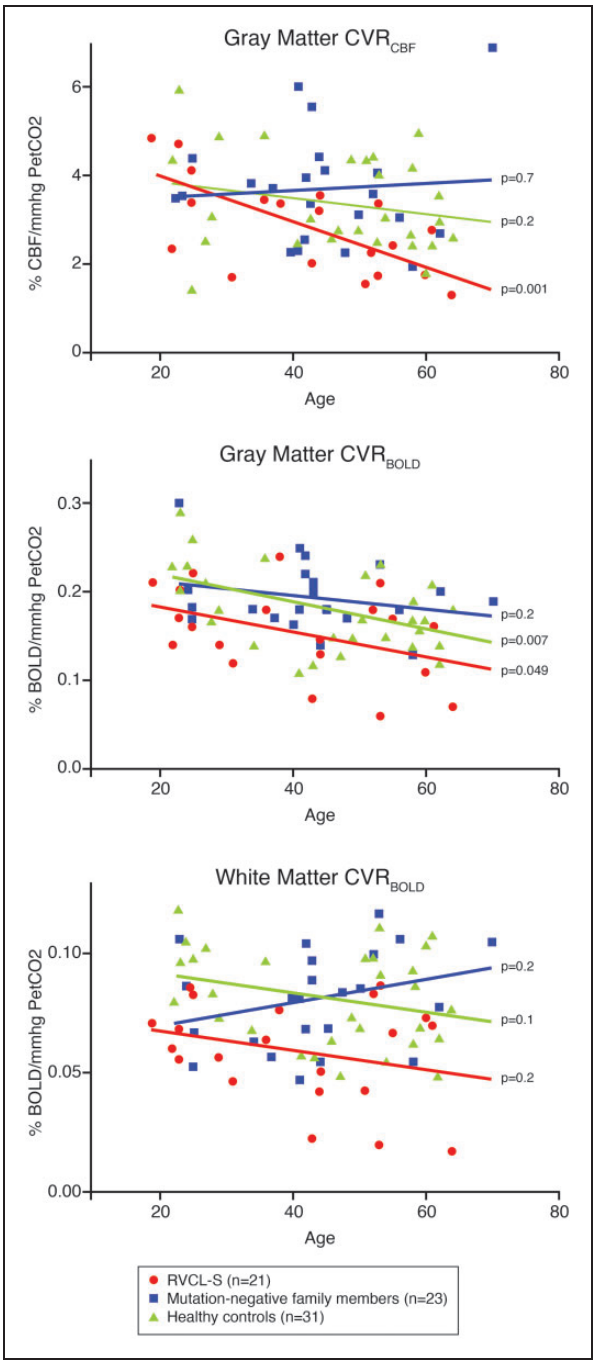

Figure 1. Cerebrovascular reactivity in relation to age in RVCL-S patients ($n = 21$), mutation-negative family members ($n = 23$), and healthy controls ($n = 31$).
CBF: cerebral blood flow; $PetCO_2$: partial pressure of end tidal CO_2; CVR: cerebrovascular reactivity; BOLD: blood oxygenation level dependent; RVCL-S: Retinal Vasculopathy with Cerebral Leukoencephalopathy and Systemic manifestations.

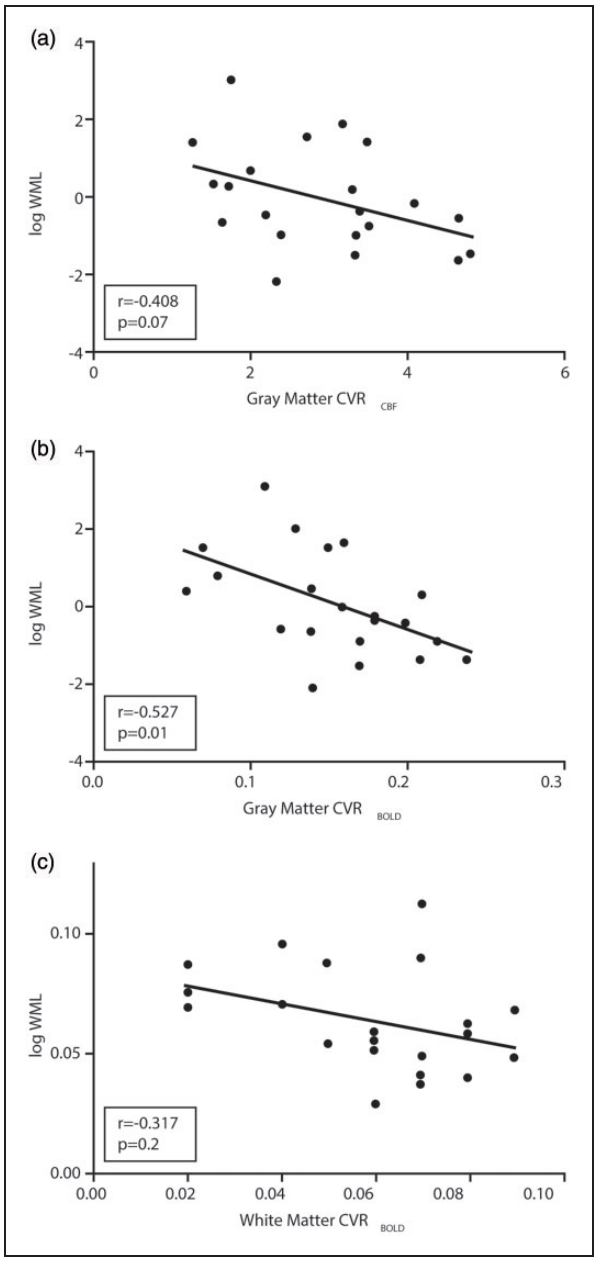

Figure 2. Correlation of white matter lesion volume with cerebrovascular reactivity in RVCL-S patients ($n = 21$).
WML: white matter lesion; CVR: cerebrovascular reactivity.

voxel-wise CVR_{CBF} and CVR_{BOLD} statistical maps but there are also some regional differences. This may be attributed to the higher signal-to-noise ratio of BOLD. Moreover, in a previous study in healthy subjects with a hypercapnic challenge, regional differences were shown between CVR_{BOLD} and CVR_{CBF}. Both measures correlated well in the frontal and temporal region, but were different in the parietal and occipital regions, probably reflecting the regionally distinct physiology of ASL and BOLD.[21]

In Figure 1, we show that gray matter CVR_{BOLD} but not white matter CVR_{BOLD} decreased significantly with age in healthy controls, which is consistent with a previous study in healthy subjects.[22] In RVCL-S patients,

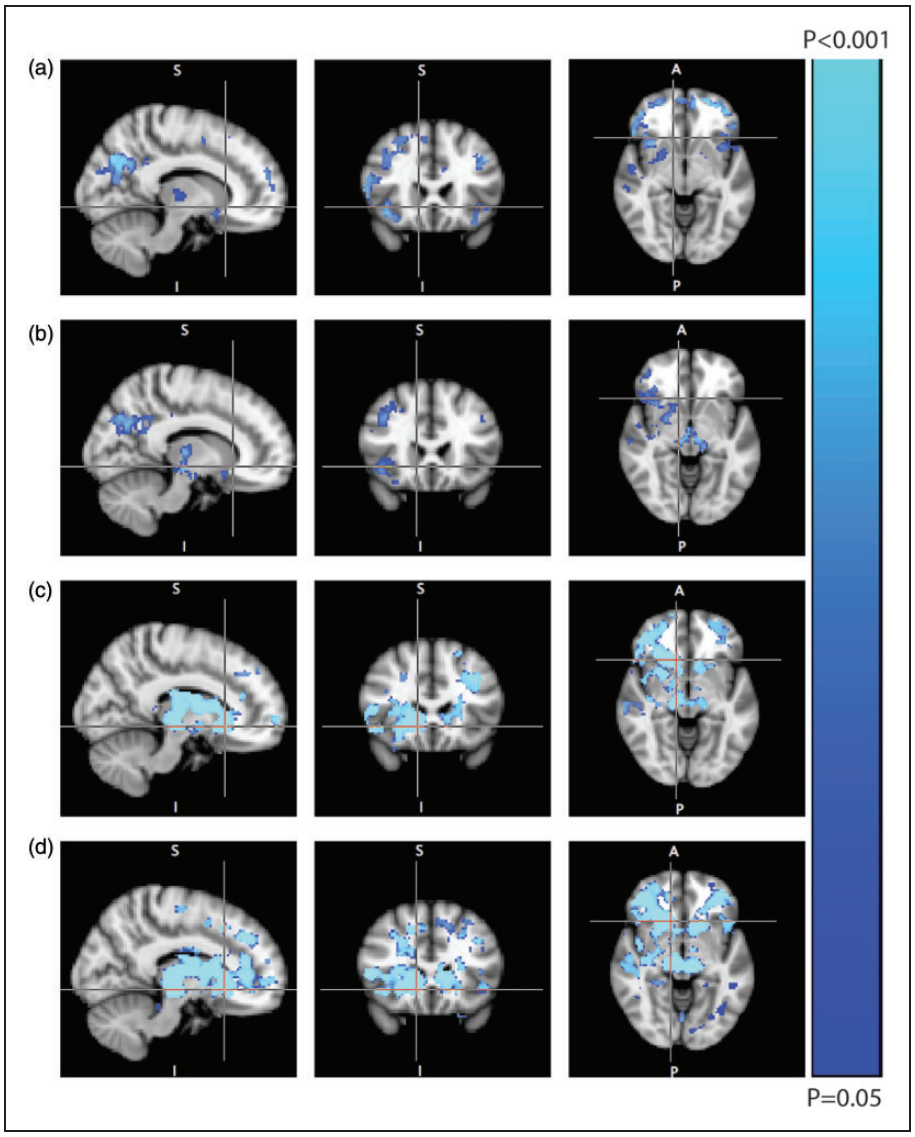

Figure 3. Voxel-wise comparison of cerebrovascular reactivity for RVCL-S patients ($n = 21$), mutation-negative family members ($n = 23$), and healthy controls ($n = 31$). (a) Regions of decreased gray matter CVR_{CBF} in RVCL-S patients versus mutation-negative family members; (b) regions of decreased gray matter CVR_{CBF} in RVCL-S patients versus healthy controls; (c) regions of decreased CVR_{BOLD} in RVCL-S patients versus mutation-negative family members; and (d) regions of decreased CVR_{BOLD} in RVCL-S patients versus healthy controls.
Note: There were no regions of increased CVR in RVCL-S patients compared to the other groups. There were no differences in CVR between mutation-negative family members and healthy controls.

gray matter CVR_{BOLD} also decreased with age, which can also be explained by advancing disease.

Strengths of this study include a unique sample of patients with RVCL-S that can be considered as a model for stroke and vascular dementia. Furthermore, to improve the accuracy of ASL-derived CBF measurements, the T1-relaxation time of blood was individually modeled as opposed to a fixed value in order to correct for differences in hematocrit.[10] Our study also has some limitations. Because RVCL-S is a rare disease, the sample size is relatively small. Moreover, it is difficult to define RVCL-S patients as asymptomatic versus symptomatic due to the many systemic features that may be part of the disease. Therefore, we chose to stratify by the age of 40, when clinical symptoms usually manifest.[2,6] Finally, due to the cross-sectional design, we cannot prove a causal relationship between CVR and WML volume in RVCL-S patients. Future

longitudinal studies are therefore required to assess whether reduced CVR is a determinant of WML progression in RVCL-S.

Conclusions

In conclusion, RVCL-S patients are associated with impaired CVR, a marker for cerebrovascular reserve capacity and cerebrovascular health. Moreover, gray matter CVR was inversely associated with brain WML volume in RVCL-S patients. These results further confirm the important role of the underlying vasculopathy in the pathophysiology of RVCL-S. CVR may be a useful early biomarker of disease severity. Future longitudinal studies are needed to assess whether CVR predicts development of typical brain RVCL-S lesions.

Funding

The author(s) disclosed receipt of the following financial support for the research, authorship, and/or publication of this article: This work was supported by grants of the Netherlands Organization for Scientific Research (NWO) (VIDI 91711319 to GMT) and the European Community (EC) (FP7-EUROHEADPAIN—no. 602633 to GMT); the funding agencies had no role in the design or conduct of the study.

Declaration of conflicting interests

The author(s) declared the following potential conflicts of interest with respect to the research, authorship, and/or publication of this article: ESH, NP, EG, AD, and MCK report no disclosures; MJPO reports speaker honoraria from Philips and independent support from NWO Domain Applied and Engineering Sciences, the European Community, and the Dutch Heart Foundation; and GMT reports independent support from NWO, ZonMW, European Community, Dutch Heart Foundation, and Dutch Brain Foundation.

Authors' contributions

ESH contributed to the conception and design of the study, data acquisition, analysis, and interpretation of the data, and drafting the manuscript; NP contributed to the conception and design of the study, data acquisition, and revising the manuscript; EG contributed to the design of the study, analysis and interpretation of the data, and revising the manuscript; MJPO contributed to the design of the study, analysis and interpretation of the data, and revising the manuscript; AD contributed to the design of the study and revising the manuscript; and GMT contributed to the conception and design of the study, interpretation of the data, and revising the manuscript; MCK contributed to the conception and design of the study, analysis and interpretation of the data, and revising the manuscript.

ORCID iDs

Evelien S Hoogeveen https://orcid.org/0000-0003-2844-4669
Matthias JP van Osch https://orcid.org/0000-0001-7034-8959

References

1. Richards A, Van den Maagdenberg AM, Jen JC, et al. C-terminal truncations in human 3'-5' DNA exonuclease TREX1 cause autosomal dominant retinal vasculopathy with cerebral leukodystrophy. *Nat Genet* 2007; 39: 1068–1070.
2. Stam AH, Kothari PH, Shaikh A, et al. Retinal vasculopathy with cerebral leukoencephalopathy and systemic manifestations. *Brain* 2016; 139: 2909–2922.
3. Jen J, Cohen AH, Yue Q, et al. Hereditary endotheliopathy with retinopathy, nephropathy, and stroke (HERNS). *Neurology* 1997; 49: 1322–1330.
4. Terwindt GM, Haan J, Ophoff RA, et al. Clinical and genetic analysis of a large Dutch family with autosomal dominant vascular retinopathy, migraine and Raynaud's phenomenon. *Brain* 1998; 121: 303–316.
5. Kolar GR, Kothari PH, Khanlou N, et al. Neuropathology and genetics of cerebroretinal vasculopathies. *Brain Pathol* 2014; 24: 510–518.
6. Pelzer N, Hoogeveen ES, Haan J, et al. Systemic features of retinal vasculopathy with cerebral leukoencephalopathy and systemic manifestations: a monogenic small vessel disease. *J Intern Med* 2019; 285: 317–332.
7. De Boer I, Stam AH, Buntinx L, et al. RVCL-S and CADASIL display distinct impaired vascular function. *Neurology* 2018; 91: e956–e963.
8. Blockley NP, Driver ID, Francis ST, et al. An improved method for acquiring cerebrovascular reactivity maps. *Magn Reson Med* 2011; 65: 1278–1286.
9. Yezhuvath US, Uh J, Cheng Y, et al. Forebrain-dominant deficit in cerebrovascular reactivity in Alzheimer's disease. *Neurobiol Aging* 2012; 33: 75–82.
10. Varela M, Hajnal JV, Petersen ET, et al. A method for rapid in vivo measurement of blood T1. *NMR Biomed* 2011; 24: 80–88.
11. Alsop DC, Detre JA, Golay X, et al. Recommended implementation of arterial spin-labeled perfusion MRI for clinical applications: a consensus of the ISMRM perfusion study group and the European consortium for ASL in dementia. *Magn Reson Med* 2015; 73: 102–116.
12. Jenkinson M, Beckmann CF, Behrens TE, et al. FSL. *Neuroimage* 2012; 62: 782–790.
13. Kitazono T, Faraci FM, Taguchi H, et al. Role of potassium channels in cerebral blood vessels. *Stroke* 1995; 26: 1713–1723.
14. Nelson MT and Quayle JM. Physiological roles and properties of potassium channels in arterial smooth muscle. *Am J Physiol* 1995; 268: C799–C822.
15. Lavi S, Gaitini D, Milloul V, et al. Impaired cerebral CO2 vasoreactivity: association with endothelial

dysfunction. *Am J Physiol Heart Circ Physiol* 2006; 291: H1856–H1861.
16. Pelzer N, Bijkerk R, Reinders MEJ, et al. Circulating endothelial markers in retinal vasculopathy with cerebral leukoencephalopathy and systemic manifestations. *Stroke* 2017; 48: 3301–3307.
17. Settakis G, Pall D, Molnar C, et al. Cerebrovascular reactivity in hypertensive and healthy adolescents: TCD with vasodilatory challenge. *J Neuroimaging* 2003; 13: 106–112.
18. Vorstrup S, Lass P, Waldemar G, et al. Increased cerebral blood flow in anemic patients on long-term hemodialytic treatment. *J Cereb Blood Flow Metab* 1992; 12: 745–749.
19. Gasparovic C, Qualls C, Greene ER, et al. Blood pressure and vascular dysfunction underlie elevated cerebral blood flow in systemic lupus erythematosus. *J Rheumatol* 2012; 39: 752–758.
20. Grand MG, Kaine J, Fulling K, et al. Cerebroretinal vasculopathy. A new hereditary syndrome. *Ophthalmology* 1988; 95: 649–659.
21. Zhou Y, Rodgers ZB and Kuo AH. Cerebrovascular reactivity measured with arterial spin labeling and blood oxygen level dependent techniques. *Magn Reson Imaging* 2015; 33: 566–576.
22. Bhogal AA, De Vis JB, Siero JCW, et al. The BOLD cerebrovascular reactivity response to progressive hypercapnia in young and elderly. *Neuroimage* 2016; 139: 94–102.